On the Application of Circular Arrays in Direction Finding Part I: Investigation into the estimation algorithms

C. M. Tan[1,†], P. Fletcher[2], M. A. Beach[1], A. R. Nix[1], M. Landmann[3], and R. S. Thomä[3]

[1]Centre for Communications Research,
Dept. Electrical and Electronic Eng.,
University of Bristol,
Bristol BS8 1UB, UK.
Tel: +44 117 954 5202
Fax: +44 117 954 5206

[2]QinetiQ
St. Andrew's Road, Malvern,
Worcs, WR14 3PS,
UK.
Tel: +44 117 954 5390
Fax: +44 117 954 5206

[3]Technical University Ilmenau,
Dept. Communication and Measurement,
P.O. Box 100565,
98684 Ilmenau, Germany.
Tel: +49 3677 69 1157
Fax: +49 3677 69 1113

[†]Email: Chor.Min.Tan@bristol.ac.uk

ABSTRACT

The performance of different direction finding algorithms for the circular arrays is investigated in this paper. Several direction estimation algorithms are studied with their pros and cons discussed. Special consideration is given to the necessary conditions needed prior to applying the algorithms in order to guarantee high accuracy in the field. Their performance is evaluated based on a simplified data model with some further assumptions, and followed by a top level comparison between each of the algorithms. The on-going research shows that the performance of the SAGE is superior to any of the other algorithms considered here when applied to a circular array.

I. INTRODUCTION

Numerous research activities have focused on evaluating the spatial characteristics of the radio channel such that antenna array based systems can be optimised during design. One of the major parameters available from the spatial domain is that of directional information, thus estimating the direction-of-arrival (DoA) or direction-of-departure (DoD) of multipaths has received considerable attention.

Different direction finding techniques and algorithms have been developed leading to significant improvements in DoA estimation over the last decade. However, to date, most of the reported algorithms are based on the uniform linear array (ULA) and the uniform rectangular array (URA) architectures, and very little attention has been given to the circular array topologies despite of their ability to offer a number of advantages. A uniform circular array (UCA) is able to provide 360º azimuthal coverage and a certain degree of source elevation information (depending on its element beampattern). Note that a URA with non-omnidirectional elements is not able to provide full azimuthal coverage due to the directional beampattern of its elements. In a beamforming application, the directional patterns of a UCA can be electronically rotated throughout the azimuth without significant change in the beam shape. All elements on the UCA will exhibit identical beampattern since the UCA has no edge elements and is less sensitive to the mutual coupling effects (compared to ULA and URA).

In terms of radio propagation, especially in a multipath-rich environment, the signals will arrive at the mobile terminal potentially from any azimuth direction. Using a ULA in a channel sounding campaign in this case will restrict the azimuth field of view to less than 180º (typically 120º). A short-term solution to this is to use several ULAs arranged in a triangular or rectangular shape (Figure 1), or to rotate the ULA a few times in order to cover the full azimuth spread. However, the drawback for the former solution is the requirement of using several ULAs (hence increasing the cost) as well as collecting additional data. While in latter solution, the time for recording the full azimuth responses will be more than the coherence time of a non-stationary channel. Obviously, the problem becomes more complicated in a double-directional measurement needed to simulate the ad-hoc channel where each mobile terminal will also act as a basestation and full azimuthal coverage is required at both ends.

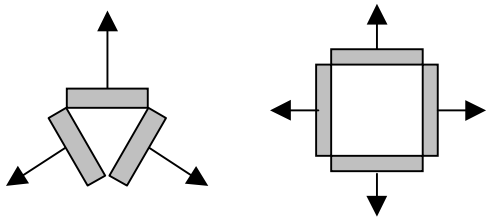

Figure 1 Triangular and rectangular arrangement of the ULAs, each covering 120º and 90º field of view

Therefore, the UCA plays an important role and its application in direction finding is investigated in this paper. Part I of this paper is organised as follows. A brief study on the UCA phase-mode excitation is given in Section 2. Section 3 investigates the pros and cons of several DoA estimation algorithms, followed by the general discussions on various issues in Section 4. Finally, Section 5 concludes Part I. In Part II [1], we evaluate the performance of the Space-Alternating Generalised Expectation-maximisation (SAGE) algorithm with real measurement data using different UCAs.

II. PHASE-MODE EXCITATION[1]

Since the beampattern of the UCA is periodic in azimuth, it can be broken down into different Fourier harmonics by using the Fourier analysis. Each of these Fourier harmonics is termed a phase-mode of the UCA [2]. The phase-mode excitation is able to transform the UCA array manifold (in the element space) into the ULA-like manifold in the UCA's phase-mode space [3]. Thus, most of the normal ULA signal processing methods (e.g. Butler beamforming matrices) can be applied to the UCA in the phase-mode domain provided certain conditions are met.

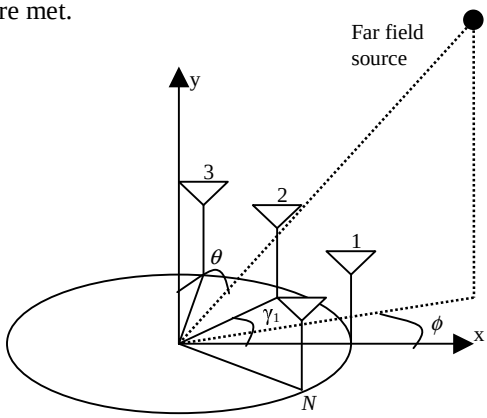

Figure 2 Uniform circular array geometry

Figure 2 shows the geometry of an *N*-element omni-directional UCA, where $\gamma_n = 2\pi n/N$, θ and ϕ are the source polar and azimuth angles measured from the *y* and *x* axis, respectively. Taking the centre of the UCA as reference, the phase shift experienced by the *n*-th element caused by a far field source is given by

$$a_n(\Theta) = e^{jk_0 r \sin\theta \cos(\phi - \gamma_{n-1})} \qquad (1)$$

$n \in [1,N]$, and the array steering vector is

$$a(\Theta) = [a_1(\Theta), a_2(\Theta), \cdots\cdots, a_N(\Theta)]^T \qquad (2)$$

where *T* denotes the vector transposition, *r* is the UCA radius, $k_0 = 2\pi/\lambda$, λ is the wavelength of the radiated signal, and $\Theta = (\theta, \phi)$.

The UCA can be excited with *m*-th phase-mode by using a *m*-th phase-mode beamforming vector, w_m:

$$w_m = \frac{1}{N}\left[e^{-jm\gamma_0}, e^{-jm\gamma_1}, \ldots\ldots, e^{-jm\gamma_{N-1}}\right]^T \qquad (3)$$

The resulting *m*-th phase-mode array beampattern is

$$f_m(\Theta) = w_m^H a(\Theta) = \frac{1}{N}\sum_{n=0}^{N-1} e^{jm\gamma_n} e^{jk_0 r \sin\theta \cos(\phi - \gamma_n)} \qquad (4)$$

where *H* denotes the Hermitian transpose operator. Using the theorem of the Bessel function,

$$e^{j\beta\cos\alpha} = \sum_{m=-\infty}^{\infty} j^m J_m(\beta) e^{jm\alpha} \qquad (5)$$

where $J_m(\beta)$ denotes a Bessel function of the first kind of order *m* with argument β, (4) can be rewritten as

$$f_m(\Theta) = j^m J_m(k_0 r \sin\theta) e^{jm\phi} + \Delta f_m(\Theta) \qquad (6)$$

where the distortion term, Δf_m, is given by

$$\Delta f_m(\Theta) = \sum_{q=1}^{\infty}\begin{pmatrix} j^g J_g(k_0 r \sin\theta) e^{-jg\phi} + \ldots \\ \ldots j^h J_h(k_0 r \sin\theta) e^{-jh\phi} \end{pmatrix} \qquad (7)$$

where $g = Nq-m$ and $h = Nq+m$.

Note that the original work in phase-mode excitation was based on a circular array with continuous aperture and its *m*-th phase-mode beampattern is given by (6) without the distortion term. For the case of a UCA with discrete elements, since only the first term in (6) is useful, every effort has been made to minimise the distortion term (7) and this has imposed some restrictions in the direction finding algorithms based on the phase-mode excitation.

Two important rules of thumb when applying phase-mode excitation to an *N*-element UCA:

1. From the property of the Bessel function (Figure 3), $J_m(\beta)$ has a small value when $|m|>\beta$. In order to excite the UCA with a reasonable strength using the highest mode *M*, *M* must be $M \approx k_0 r \sin\theta \in [0, k_0 r]$ and the maximum mode is given by the smaller integer that is closer to or equal to $k_0 r$. Hence, the modes that can be excited are $m \in [-M, M]$.

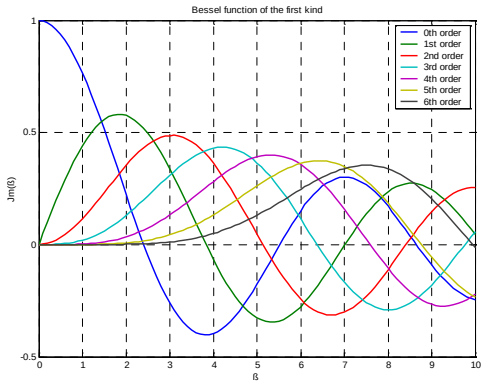

Figure 3 Bessel function of the first kind

2. From the spatial Nyquist sampling theorem, the UCA circumferential sampling rate should be at least twice the highest spatial frequency present in the array excitation [2]. Therefore, in order to reproduce all the spatial harmonics that are

[1] The concept of the phase-mode excitation of a UCA was introduced in the 1960s and had been studied in great depth by Davies [2][3].

excited, the number of elements in the UCA must satisfy $N \geq 2M$.

Note that these two conditions decide the appropriate radius and number of elements of the UCA, and thus set the largest circumferential spacing between the adjacent UCA elements to be $\lambda/2$, and $r_{\max} = \frac{N\lambda}{4\pi}$.

III. INVESTIGATION INTO DIFFERENT DIRECTION FINDING ALGORITHMS

This section investigates several direction finding algorithms using a UCA. To aid the following discussions, we begin by constructing a common narrowband signal model used in the estimation algorithms. Assuming a total of *K* sources impinging on an *N*-element omni-directional UCA, the array response can be represented by

$$x(t) = As(t) \qquad (8)$$

where $A = [a(\Theta_1) : a(\Theta_2) : \cdots\cdots : a(\Theta_K)]$ is the array response matrix, and $s(t) = [s_1(t), s_2(t), \cdots\cdots, s_K(t)]^T$ represents the *K* far field sources. In order to simplify the studies, it is assumed that the number of sources is known, the sources are uncorrelated, the channel is noiseless, and the sources lie in the azimuth plane, i.e. $\theta = 90^o$ and $\Theta \equiv \phi$.

A number (*p*) of array snapshots are collected within the coherence time of the channel and the data matrix is given by

$$X = [x(t_1) : x(t_2) : \cdots\cdots : x(t_p)] \qquad (9)$$

The expected covariance matrix, *R*, is thus defined as

$$R = \frac{1}{p} XX^H \qquad (10)$$

A. The Classical Beamforming Method (CBM)

The CBM is the simplest direction finding algorithm. It estimates the DoA of the signals by scanning a beam throughout the azimuth, and the DoAs are located by the peaks in the power azimuth spectrum, $P_{CBM}(\phi)$, given by

$$P_{CBM}(\phi) = a^H(\phi) R a(\phi) \qquad (11)$$

Similar to the ULA's case, the performance of CBM is limited by the Rayleigh resolution and is not able to resolve the closely spaced signals.

B. Capon's Beamforming Method (Min-Variance)

The Capon's Beamforming [4] method is also known as the Minimum Variance Distorsionless Response (Min-Variance). It is similar to the CBM, with an additional feature of minimising the power contributed by signals from other direction while maintaining a fixed gain in the look direction. Although its resolution is better than CBM, it is still dependent upon the number of elements and the signal-to-noise ratio (SNR) of the channel. Its power azimuth spectrum is given by

$$P_{MV}(\phi) \frac{1}{a^H(\phi) R^{-1} a(\phi)} \qquad (12)$$

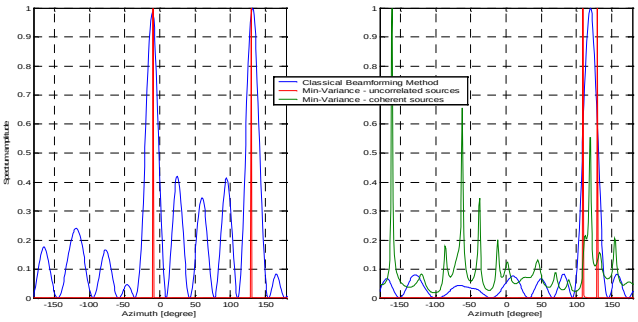

a *b*

a – 2 equipower uncorrelated sources at -10º and 130º
Classical Beamforming Method, Min-Variance

b – 2 equipower sources at 110º and 130º
Classical Beamforming Method (uncorrelated sources)
Min-Variance (uncorrelated sources)
Min-Variance (sources are coherent)

16-element omni-directional UCA, r=λ

Figure 4 Power spectrums of the CBM and Min-Variance algorithm

Figure 4 (details in caption) demonstrates the poor resolution of the CBM that is not able to resolve closely spaced sources. The high sidelobes of the CBM also leads to misleading results. Although Min-Variance has high-resolution, it fails when the sources are coherent.

C. MUltiple SIgnal Classification (MUSIC)

C.1. Conventional MUSIC in element space

Although the element space MUSIC algorithm introduced by Schmidt [5] has been widely used with a ULA, it can also be used with a UCA, provided that the sources are uncorrelated and the knowledge of array manifold is available. Using the eigen-decomposition procedure explained in [5], the MUSIC spectrum is given by

$$P_{MU}(\phi) = \frac{1}{a^H(\phi) E E^H a(\phi)} \qquad (13)$$

where *E* is the noise subspace of *R* in (10), and $a(\phi)$ is defined in (2).

C.2. MUSIC in phase-mode space

When the sources are coherent, the covariance matrix *R* is rank deficient and spatial smoothing technique

must be applied prior to applying any eigen-decomposition based algorithm. However, the original development of the spatial smoothing technique [6] was based on the Vandermonde structure in the steering vector of a ULA. UCA phase-mode excitation provides a means to restore the Vandermonde structure in the UCA steering vector (2), with the penalty of reduced aperture size in the phase-mode space.

C.2.1. Standard implementation

The element space data matrix, X, can be transformed into the phase-mode space by

$$X_{pm} = JF^H X \qquad (14)$$

where

$$J = diag\left\{\frac{1}{\sqrt{N}\, j^m J_m(k_0 r)}\right\} \; m \in [-M, M] \qquad (15)$$

and $$F = [w_{-M} \vdots \cdots\cdots \vdots w_0 \vdots \cdots\cdots \vdots w_M] \qquad (16)$$

is the phase-mode beamforming matrix. At this stage, the UCA spatial smoothing [7] technique can be applied to the new phase-mode space data (14).

For simplicity, without applying the phase-mode spatial smoothing, the MUSIC spectrum is given by

$$P_{pm}(\phi) = \frac{1}{a_{pm}^H(\phi) E_{pm} E_{pm}^H a_{pm}(\phi)} \qquad (17)$$

where E_{pm} is the phase-mode space noise-subspace, and $a_{pm}(\phi) = JF^H a(\phi)$ is the phase-mode steering vector that exhibits the Vandermonde structure.

Note that the Bessel function term, $J_m(.)$, has been included in the computation of J in (15), since we have assumed $\theta = 90^o$ here. However, as $\theta \neq 90^o$ in practice, $J_m(.)$ would not be included in (15) so that θ can be estimated as well.

C.2.2. UCA-RB-MUSIC

The UCA Real Beamspace MUSIC (UCA-RB-MUSIC) introduced by Mathews and Zoltowski [8] transforms the data matrix and the array manifold into their real-valued counterparts in phase-mode space by using a unitary matrix W (refer to [8] for the construction of W). Due to the property of W, UCA-RB-MUSIC effectively works with a forward-backward averaged covariance matrix. Hence, its performance is more robust when dealing with two correlated sources. However, when more than two sources are correlated, spatial smoothing [7] must be applied. In addition, in the case of estimating both θ and ϕ, the speed of locating the peaks in its 2-D spectrum can be accelerated with the aid of a FFT process (more details in [8]).

C.2.3. Unitary UCA-MUSIC

Note that the noise subspace in the UCA-RB-MUSIC is determined from the real part of the calculated covariance matrix. This is rather confusing since the computation in UCA-RB-MUSIC is accomplished in real-valued space. The authors [8] had claimed that the UCA-RB-MUSIC is implemented in real-valued since its imaginary part is nearly zero, i.e. almost real. In order to fully eliminate the imaginary part to facilitate the real-valued eigen-decomposition, the authors had ignored the 'nearly-zero' imaginary part of the covariance matrix. To some small extent, this leads to minor leakage of some useful information associated with the imaginary part.

Enhancement can be made by using the unitary left Π-real matrix defined in [9] – 'Q', to convert the complex-valued data matrix into its real-valued counterpart in phase-mode space. Hence, the eigen-decomposition of the covariance matrix in Unitary UCA-MUSIC can be performed in a true real-valued domain. Similarly, the forward-backward averaging process has been incorporated in this process and hence, the Unitary UCA-MUSIC is also robust in resolving two correlated sources.

C.3. Simple demonstration on MUSIC

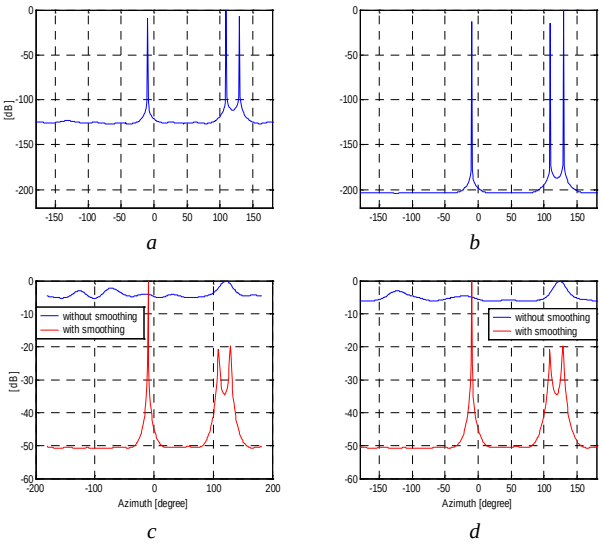

a – spectrum of UCA-RB-MUSIC
b – spectrum of Unitary UCA-MUSIC
c – spectrums of phase-mode space MUSIC
d – spectrums of Unitary UCA-MUSIC

16-element omni-directional UCA, r = λ
without smoothing, with smoothing
a, b – 3 equipower uncorrelated sources at -10º, 110º, 130º
c, d – 3 equipower coherent sources at -10º, 110º, 130º

Figure 5 Spectrums of various MUSIC algorithms

From the spectrums of UCA-RB-MUSIC and Unitary UCA-MUSIC algorithms shown in Figures 5a and 5b respectively (details in caption), the performance of UCA-RB-MUSIC is inferior to that

of Unitary UCA-MUSIC since the latter has a lower noise floor. Nevertheless, both algorithms have successfully produced the correct estimates and the peaks corresponding to the three sources can be easily located. The total failure of the algorithms without spatial smoothing shown in Figures 5c and 5d demonstrates that spatial smoothing process must be performed when the sources are coherent.

D. Estimation of Signal Parameters via Rotational Invariance Techniques (ESPRIT)

One strict condition imposed by ESPRIT [10] is the presence of two identical, translationally invariant subarrays. Although we can define two such subarrays from a UCA, Swindlehurst [11] showed that the original ESPRIT [10] algorithm applied to UCA fails when more than one source is present. Therefore, special modifications must be performed if ESPRIT were to be used with a UCA.

D.1. UCA-ESPRIT

Mathews and Zoltowski [8][12] had proposed the UCA-ESPRIT algorithm based on the concept of recursive relationship of the Bessel functions:

$$J_{m-1}(\beta)+J_{m+1}(\beta)=\frac{2m}{\beta}J_m(\beta) \qquad (18)$$

Although its implementation is a little different from the original ESPRIT, it is similar in the sense that a Least Squares solution must be performed on a set of overdetermined equations before the signal parameters are obtained from its eigenvalues. The main advantage of UCA-ESPRIT is its ability to provide automatically paired θ and ϕ as a closed-form solution. However, in a non-coherent case, the maximum number of sources that can be resolved is M-1, i.e. less than half of the resolution of MUSIC. Moreover, its estimates are also a little biased. Hence, the authors had proposed to use the UCA-ESPRIT to provide a coarse estimate to initialise the search function of the MUSIC in order to increase the convergence speed of the MUSIC's peak-searching routine.

Table 1 shows the results of UCA-ESPRIT under different conditions (details in caption). The number of sources that can be resolved by UCA-ESPRIT when N = 8 is 2, since $M_{(N=8)}$ = 3. By using a UCA with more elements, the number of resolvable sources can be increased and the estimates are also more accurate, since the degree of freedom is higher. This is shown in Table 1 where the estimated results when N = 16 are more accurate. In addition, by using a UCA with its radius smaller than the upper bound limit stated in Section 2, i.e. circumferential spacing between adjacent elements of less than $\lambda/2$, the accuracy of the estimates can also be improved.

N	r [λ]	$(\theta_1, \phi_1) = (75^o, 110^o)$ $(\theta_2, \phi_2) = (90^o, 130^o)$
8	0.63	$\Theta_{e1} = (45^o, 108.7^o)$ $\Theta_{e2} = (90^o, 125.5^o)$
	0.50	$\Theta_{e1} = (72^o, 105.0^o)$ $\Theta_{e2} = (90^o, 126.6^o)$
16	1.27	$\Theta_{e1} = (69^o, 108.7^o)$ $\Theta_{e2} = (90^o, 135.5^o)$
	1.00	$\Theta_{e1} = (78^o, 110.8^o)$ $\Theta_{e2} = (90^o, 131.3^o)$

N-element omni-directional UCA with r radius [in terms of λ]
2 equipower uncorrelated sources at (75º, 110º) and (90º, 130º)
Estimated direction is shown in third column by Θ_{e1} *and* Θ_{e2}

Table 1 Estimated results using UCA-ESPRIT

D.2. Unitary UCA-ESPRIT in phase-mode space

Similar to the UCA-RB-MUSIC, the process of eigen-decomposition of the covariance matrix in UCA-ESPRIT has ignored the 'nearly-zero' imaginary part of its covariance matrix. In order to facilitate a true real-valued computation, and to improve the resolution of UCA-ESPRIT, the Unitary UCA-ESPRIT in phase-mode space is proposed here.

The implementation of Unitary UCA-ESPRIT is based on the combined concept of phase-mode excitation and Unitary ESPRIT [9] algorithm. Similar to the Unitary UCA-MUSIC algorithm, the new introduced step in Unitary UCA-ESPRIT involves the transformation of the phase-mode space data matrix (14) from its complex space to its real-valued counterpart by using the unitary left Π-real matrix defined in [9] – 'Q', and followed by the ordinary Unitary ESPRIT procedure in the subsequent steps. This results in increased accuracy compared to UCA-ESPRIT, and increased number of resolvable uncorrelated sources from M-1 to 2M.

However, since the θ-dependent term, i.e. the Bessel function, has been eliminated by J (15) in X_{pm} (14), only azimuth angle can be estimated using the Unitary UCA-ESPRIT algorithm. This also suggests a degradation in the performance of Unitary UCA-ESPRIT if $\theta \neq 90^o$, and from the extensive simulation results, Unitary UCA-ESPRIT fails when $\theta < 70^o$. This implies that although the performance of Unitary UCA-ESPRIT is superior to UCA-ESPRIT when $\theta = 90^o$, UCA-ESPRIT would still be the preferred choice since $\theta \neq 90^o$ in practice.

D.3. CUBA-ESPRIT

The CUBA-ESPRIT [13] was specially developed for direction finding using a circular uniform beam array [14] (CUBA). Its implementation requires that the element beampattern of the array exhibit a $sinc(x)$ function, or more precisely the beam spectrum must

be bandlimited. Figure 6 shows the beampattern of an 8-element CUBA and one of its elements. Due to the unique feature of this *sinc*(*x*)-shape pattern, the CUBA element space data can be transformed into a virtual aperture domain by an FFT process, in which the shift invariance property of the ESPRIT is fully restored, and the spatial smoothing process can thus be applied. This advantage is achieved at a cost of a smaller virtual aperture size and hence a reduction in the total number of resolvable sources.

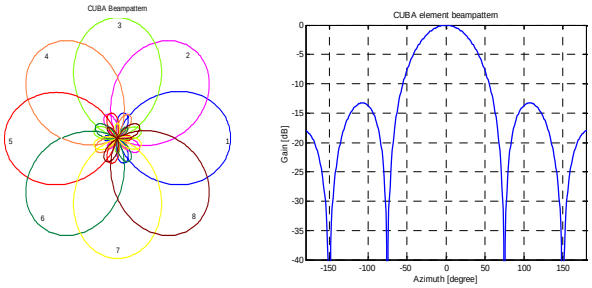

a *b*

a – 8-element CUBA beampattern
b – Beampattern for the 1st element

Figure 6 CUBA beampattern

For the case of a UCA, if the beampattern does not exhibit the appropriate *sinc*(*x*) function, a *sinc*(*x*) beamforming procedure can be performed prior to implementing the CUBA-ESPRIT. However, due to all sorts of array imperfections, a perfect *sinc*(*x*)-shape beampattern could not be synthesised even after the beamforming procedure and this leads to increased bias and errors in the estimation.

In addition, CUBA-ESPRIT assumes that there is no additional phase shift at the element-outputs, i.e. a common phase centre for all elements. This implies that the UCA must have very small diameter (ideally zero) like that of a CUBA, which is practically impossible for a normal UCA. Although CUBA-ESPRIT has been proven to be very efficient and robust, it is only suitable for a CUBA but not for other ordinary UCAs, especially for those with directional element beampattern.

E. Space-Alternating Generalised Expectation-maximisation (SAGE)

Similar to the Expectation-Maximisation (EM) algorithm [15], the SAGE algorithm [16][17] is a maximum-likelihood (ML) based algorithm and its implementation is very different from the aforementioned algorithms that rely on eigen-decomposition. Neither does SAGE need to fulfill the rotational invariance characteristic of ESPRIT, nor to exploit the array Vandermonde structure, since spatial smoothing process is not required in SAGE even when the sources are correlated. The principal advantage of SAGE is its flexibility in any array geometry and hence can be applied to any arbitrary array (in theory), provided the knowledge of the array manifold is fully available. However, one major drawback is its slow convergence since it is iterative in nature.

The objective of the SAGE algorithm is to maximise the correlation function, defined as

$$c_k(x,\phi) = x_k^H a(\phi) \qquad (19)$$

where x_k is the *complete data* [15][16] of the *k*-th source. The peak in c_k corresponds to the location of the estimated parameter of the *k*-th source. Figure 7 shows the correlation functions of the SAGE (details in captions). Since this is a 1-D estimation process, the *Serial Interference Cancellation* (SIC) technique proposed in [17] cannot be used, especially in a case where the sources are closely spaced apart. Here, we have used the conventional *Parallel Interference Cancellation* (PIC) technique [16].

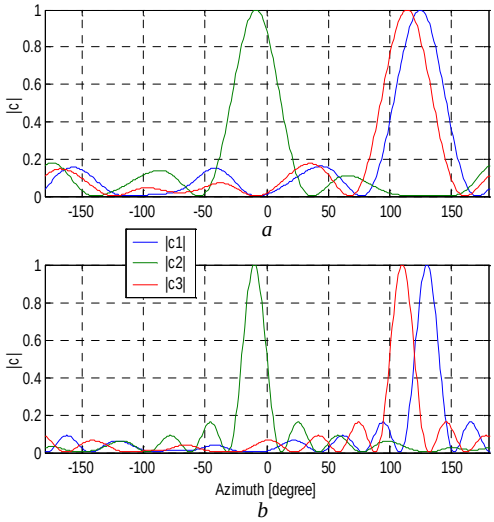

a

b

a – 8-element omni-directional UCA, r=λ/2
b – 16-element omni-directional UCA, r=λ
3 equipower coherent sources at -10º, 110º, 130º
correlation function for the 130º source
correlation function for the -10º source
correlation function for the 110º source

Figure 7 Correlation functions of the SAGE with PIC technique

As shown here, SAGE is able to cope with the coherent sources and spatial smoothing is not required. The convergence speed of SAGE depends on the degree of separation between the paths, and the number of elements used in the array, since the number of samples required in the correlation increases (more samples can enhance the accuracy of the correlation) as the number of elements increases. For a 16-element UCA, the SAGE has converged after 3 iterations, giving the correct estimates at -10º, 110º, and 130º (Figure 7b). However, for the 8-element UCA, after 3 iterations, the estimated results are -9º, 114º, and 125º (Figure 7a) and thus more iterations are needed to achieve convergence especially for the 2 sources at 110º and 130º. Note that in practice, more iterations might be needed since we have assumed a simplified model here. In

any event, as the number of samples grows, the computational load of the SAGE increases exponentially especially in a multi-dimensional case.

F. UCA-to-ULA mapping technique

The so-called '*mapping*' technique proposed by Hyberg [18] can transform the UCA data, in a Least Squares sense, into that of a virtual ULA, by a transformation matrix - T_k. The computation of T_k requires a large amount of measured array manifold data and can only map a small sector (typically 30º as recommended) of a UCA data onto the virtual ULA each time.

After the UCA-to-ULA mapping, both the θ and ϕ are estimated using the normal ULA-type algorithms separately in the transformed elevation and azimuth domains, respectively. As a result, a separate procedure must be developed to pair up both the θ and ϕ. In addition, Hyberg also reported that biased errors occur in the estimated results using this technique.

In spite of all these problems, Hyberg has claimed that using the similar mapping technique to transform a UCA data into that of a smaller virtual UCA can improve the resolution of the UCA-ESPRIT algorithm.

IV. GENERAL DISCUSSIONS

The effectiveness and performance of the estimation algorithms mainly depend on the array geometry. Most of the array signal processing techniques are based on the ULA since the important criterions needed by the algorithms can be easily fulfilled with a ULA. As such, many researchers have attempted to adapt the ULA's signal processing techniques to the UCA, with some extra procedures like the phase-mode excitation. This causes the original information associated with the UCA to be modified into another domain. However, not all information can be preserved and this leads to degradation in performance. This can be clearly observed in the estimated results of UCA-ESPRIT which is inferior to that of the UCA-MUSIC, where the performance of ESPRIT in ULA is supposed to be superior to MUSIC.

Phase-mode excitation in UCA signal processing is important because it allows the spatial smoothing process to be performed in MUSIC, and the rotational shift invariance property to be restored in ESPRIT. However, the phase-mode excitation for a UCA with discrete elements is distorted by the residue term (7) due to finite sampling around the circular aperture. As the mode being excited becomes larger, the effects caused by the distortion term (7) become more apparent. This is shown in Figure 8 for the 2nd and 7th modes of a 16-element UCA, where the contribution from the distortion term can be clearly seen in the responses of the 7th mode.

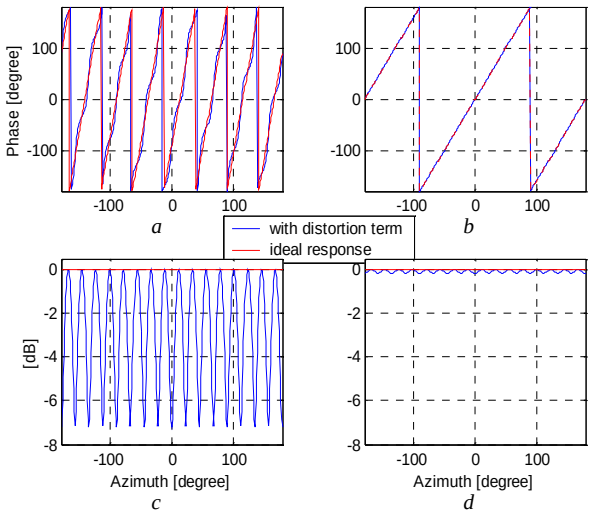

a – phase response of the 7th mode
b – phase response of the 2nd mode
c – amplitude response of the 7th mode
d – amplitude response of the 2nd mode

actual mode response, assumed ideal mode response

Figure 8 Responses of the phase-mode excitation of 16-element omni-directional UCA

In general, using a UCA with $N = 2M + 6$ elements will virtually eliminate the distortion, where M is the maximum mode to be excited [12]. This implies that in order to achieve better accuracy, the transformation from the element space into the phase-mode space has further reduced the aperture size of the data, and hence reducing the maximum number of resolvable sources. This introduces further constraints to the algorithms that a large number of elements is required so that the estimated results will be reliable.

On the other hand, although the SAGE algorithm is computationally expensive (especially in multi-dimensional parameters estimation), it has demonstrated its suitability and excellent performance when applied to a UCA. Chan [19] and Wax [7] showed that the maximum-likelihood algorithms (like SAGE) have better performance than MUSIC. Note that as long as the knowledge of the array manifold is available, SAGE will produce reliable results. The performance of other algorithms considered in this paper is inferior to that of SAGE even when the sources are uncorrelated and the channel is noiseless. One would appreciate further merits on SAGE when the simulation includes highly correlated sources, bad SNR in the channel, and by using a non-ideal UCA with directional beampattern and mutual coupling. Under such conditions, we would expect a total failure in other algorithms but it is very likely that SAGE will survive.

V. CONCLUSION

In this paper, the pros and cons of several direction finding algorithms with a UCA are investigated. The conditions that govern the performance of the algorithms are stated. The analysis shows that the SAGE algorithm is superior to other algorithms when applied to a UCA, and should be the preferred choice when the number of elements is small. Other algorithms are suitable only when the number of elements on the UCA is large, and appropriate spatial calibration algorithm must be performed to eliminate the mutual coupling effects and any array imperfection on the UCA – a process that is essential especially if ESPRIT were to be applied with a UCA.

ACKNOWLEDGEMENT

The authors would like to acknowledge Mobile VCE (www.mobilevce.com) for the financial support of Chor Min Tan.

REFERENCES

[1] C. M. Tan, M. Landmann, A. Richter, L. Pesik, M. A. Beach, Ch. Schneider, R. S. Thomä, A. R. Nix, '*On the application of circular arrays in direction finding, Part 2: Experimental evaluation on SAGE with different circular arrays*', companion paper in 1st Annual COST 273 Workshop, Espoo, Finland, May 29-30, 2002.

[2] D. E. N. Davies, '*Circular arrays*', Chap. 12, The Handbook of antenna design, London Peregrinus on behalf of the IEE, 1983.

[3] D. E. N. Davies, '*A transformation between the phasing techniques required for linear and circular aerial arrays*', Proc. IEE, Vol. 112, No. 11, Nov 1965.

[4] J. Capon, '*High resolution frequency wavenumber spectrum analysis*', Proc. IEEE, Vol. 57, No. 8, Aug 1969, pp. 1408-1418.

[5] R. O. Schmidt, '*Multiple emitter location and signal parameters estimation*', IEEE Trans. Ant. Prop., Mar 86, pp. 276-280.

[6] T. J. Shan, M. Wax, T. Kailath, '*On spatial smoothing for direction-of-arrival estimation of coherent signals*', IEEE Trans. ASSP, Vol. 33, Aug 1985, pp. 806-811.

[7] M. Wax, J. Sheinvald, '*Direction finding of coherent signals via spatial smoothing for uniform circular arrays*', IEEE Trans. Ant. Prop., Vol. 42, No. 5, May 1994, pp. 613-620.

[8] C. P. Mathews, M. D. Zoltowski, '*Eigenstructure techniques for 2-D angle estimation with uniform circular arrays*', IEEE Trans. Signal Proc., Vol. 42, No. 9, Sept 1994, pp. 2395-2407.

[9] M. Haardt, J. A. Nossek, '*Unitary ESPRIT: How to obtain increased estimation accuracy with a reduced computational burden*', IEEE Trans. Signal Proc., Vol. 43, May 1995, pp. 1232-1242.

[10] R. Roy, T. Kailath, '*ESPRIT-Estimation of Signal Parameters via Rotational Invariance Techniques*', IEEE Trans. ASSP, Vol. 37, pp. 984-995, July 1989.

[11] A. Swindlehurst, '*DOA identifiablity for rotationally invariant arrays*', IEEE Trans. Signal Proc., Vol. 40, No. 7, July 1992, pp. 1825-1827.

[12] C. P. Mathews, M. D. Zoltowski, '*Performance analysis of the UCA-ESPRIT algorithm for circular ring arrays*', IEEE Trans. Signal Proc., Vol. 42, No. 9, Sept 1994, pp. 2535-2539.

[13] A. Richter, R. S. Thomä, '*CUBA-ESPRIT for angle estimation with circular uniform beam arrays*', Proc. Millennium Conf. AP2000, Davos, Switzerland, Apr 9-14 2000.

[14] F. Demmerle, W. Wiesbeck, '*A biconical multibeam antenna for space division multiple access*', IEEE Trans. Ant. Prop., Vol. 46, No. 6, June 1998, pp. 782-787.

[15] M. Feder, E. Weistein, '*Parameter estimation of superimposed signals using the EM algorithm*', IEEE Trans. Signal Proc., Vol. 36, No. 4, Apr 1988, pp. 477-489.

[16] B. H. Fleury, M. Tschudin, R. Heddergott, D. Dahlhaus, K. I. Pedersen, '*Channel parameter estimation in mobile radio environments using the SAGE algorithm*', IEEE JSAC, Vol. 17, No. 3, Mar 1999, pp. 434-449.

[17] C. C. Chong, D. I. Laurenson, C. M. Tan, S. McLaughlin, M. A. Beach, A. R. Nix, '*Joint detection estimation of directional channel parameters using the 2-D frequency domain SAGE algorithm with Serial Interference Cancellation*', conference proceeding in ICC 2002, New York City, Apr 28- May 2 2002.

[18] P. E. Hyberg, '*Circular to linear array mapping using calibrated data*', IEE Conf. HF Radio Systems and Techniques, 2000.

[19] A. Y. J. Chan, J. Litva, '*MUSIC and maximum likelihood techniques on two-dimensional DoA estimation with uniform circular array*', IEE Proc. Radar, Sonar, Navig., Vol. 142, No. 3, June 1995, pp. 105-113.